

Pseudorotation in Radical Cations of Low-Symmetric Decalin Molecules

Irina V. Beregovaya,[†] Lyudmila N. Shchegoleva,^{*,†} and Vsevolod I. Borovkov[‡]

N. N. Vorozhtzov Novosibirsk Institute of Organic Chemistry, Novosibirsk, 630090, Russia, and Institute of Chemical Kinetics and Combustion, Novosibirsk, 630090, Russia

Received: August 25, 2008; Revised Manuscript Received: December 22, 2008

Adiabatic potential energy surfaces (PES) of isomeric decalin cations have been found to be the pseudorotational surfaces due to avoided crossing that is typical for the highly symmetric Jahn–Teller active ions rather than for low-symmetric bicyclic systems. According to the UB3LYP/6-31G* data, the height of the barrier to pseudorotation is less than 2 kcal/mol for the *trans* isomer and about 9 kcal/mol for the *cis* isomer. Another peculiarity of the *cis* isomer PES is that the structure of minimum energy lies beyond the pseudorotation gutter. The calculation results are in fair agreement with the experimental electron spin resonance data.

1. Introduction

A decalin molecule $C_{10}H_{18}$ exists as *cis* and *trans* isomers; in both the cases “chair–chair” conformations (Figure 1) are energetically favorable.¹ Radical cations (RCs) of *cis*- and *trans*-decalin have been studied in low-temperature matrices^{2–6} and zeolites⁷ as well as in liquid solutions^{8,9} using the electron spin resonance (ESR) technique and the methods of optically detected ESR (OD ESR) and magnetic field effect on reaction yield (MARY) spectroscopy, respectively. The spectral behavior of the isomeric cations proved to be significantly different. In Freon matrices, the ESR spectrum of *c*-DEC⁺⁺ depends neither on the matrix nor on the temperature.⁴ On the contrary, two different ESR spectra corresponding to $a_H = 52$ (4H) and $a_H = 36.6$ (4H) G are observed for *t*-DEC⁺⁺ depending on the matrix. Moreover, in *c*-C₆F₁₁CF₃ and CF₂CICFCCl₂ at 4.2 K both the spectra have been registered simultaneously. The spectrum observed in *c*-C₆F₁₁CF₃ at 77 K was simulated by assuming of spectral exchange with an exchange rate $k_{12} = 7.9 \times 10^7$ s⁻¹, and the 125 K spectrum corresponded to limit case of complete averaging of hyperfine coupling (hfc). These results were interpreted by Melekhov et al.⁴ using the MNDO calculations which indicated the energy closeness of two *t*-DEC⁺⁺ structures with different ground states, C_{2h} (²A_g) and C_{2h} (²B_g). INDO calculations of isotropic hfc constants for these structures reproduced well the experimental ESR data.

An essential distinction between *c*-DEC⁺⁺ and *t*-DEC⁺⁺ has been also revealed in liquid solutions.⁸ So, the resolved OD ESR spectrum of *c*-DEC⁺⁺ was observed in irradiated *cis*-decalin solution even at room temperature. Unlike that, *t*-DEC⁺⁺ was never observed in liquid solution by OD ESR method. It is in agreement with the dramatic difference in the times of spin–lattice relaxation of these RCs in solutions, $T_1 \approx 14$ ns for *t*-DEC⁺⁺ and $T_1 \approx 400$ ns for *c*-DEC⁺⁺. This difference was revealed by both the MARY spectroscopy^{8,9} and the method of time-resolved magnetic field effect.¹⁰

Substantially, when going from Freon matrices to some zeolites,⁷ the distinction in spectral behavior of the *t*-DEC⁺⁺ and *c*-DEC⁺⁺ is leveled. Two different electronic states and spectral exchange between them are observed for both RCs depending

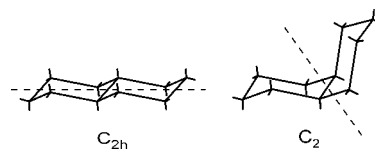


Figure 1. Isomer forms of the decalin molecule: *trans*-decalin (C_{2h}) and *cis*-decalin (C_2). The dashed line denotes the main element of the symmetry, the C_2 axis.

on particular zeolite. Apparently, in this case the energy gap of the *c*-DEC⁺⁺ states is comparable with the energy of the RC interaction with zeolite matrix.

Thus, the data provided by the ESR experiments for decalin RCs strongly suggest the existence of close in energy electronic states in these RCs. This may seemingly result in structure distortions and complicated structure of adiabatic potential energy surfaces (PES). However, PESes of these RCs have not been studied yet, and this investigation is a goal of the present work. Here we performed ab initio PES study of the *cis*- and *trans*-decalin RCs to locate the stationary structures and to determine their interrelation. Calculated hfc constants are compared with the experimental ESR data.

2. Computational Details

To obtain a qualitative view of PES structure, we have estimated the energies of vertical cation states of the *cis*- and *trans*-decalin molecules at ROHF and CIS/ROHF calculation levels and considered a possibility of intersection of the electronic states in respective RCs. The proper PES studies have been performed with the DFT UB3LYP method. The 6-31G* basis set is used in all the calculations. The types of stationary PES points have been determined by the normal vibrations analysis. Their interrelations have been found out by means of the intrinsic reaction coordinate (IRC) technique. For comparison, some calculations of the cyclohexane neutral molecule and RC have been done as well. The main calculations have been carried out by the GAMESS program package.¹¹ Some preliminary calculations of low-symmetric transition states have been performed at the PBE/3z level by the PRIRODA program¹² that allowed us to reduce computational expenses.

3. Results and Discussion

Figure 2 shows higher-occupied molecular orbitals (HOMOs) of the *cis*-decalin and *trans*-decalin molecules together with the

* To whom correspondence should be addressed. E-mail: sln@nioch.nsc.ru. Phone: +7 383 330 6859. Fax: +7 383 330 9752.

[†] N. N. Vorozhtzov Novosibirsk Institute of Organic Chemistry.

[‡] Institute of Chemical Kinetics and Combustion.

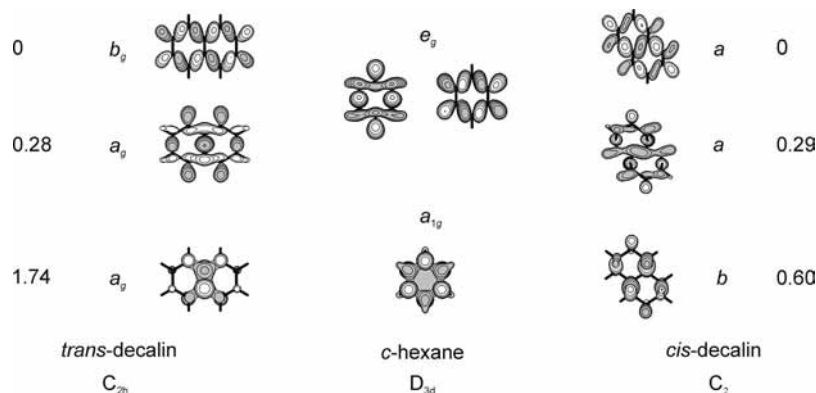


Figure 2. HOMO of the cyclohexane and isomeric decalin molecules. For *trans*- and *cis*-decalin, the relative energies (eV) of the respective vertical cation states are presented according to the data of CIS/6-31G**/ROHF/6-31G* calculations.

TABLE 1: Intersection of Lower Electronic States of *trans*- and *cis*-Decalin Radical Cations^a

radical cation	state	geometrical structure			
		ROHF/6-31G*		CIS/6-31G**/ROHF/6-31G* ^b	
<i>t</i> -DEC ⁺⁺		C_{2h} (2A_g)	C_{2h} (2B_g)	C_{2h} (2A_g)	C_{2h} (2B_g)
	2A_g	-388.880378	-388.790658	-388.919112	-388.844130
	2B_g	-388.723463	-388.843667	-388.798632	-388.930778
<i>c</i> -DEC ⁺⁺		C_2 (2A)	C_2 (2B)	C_2 (2A)	C_2 (2B)
	2A	-388.875654	-388.778032	-388.914733	-388.858063
	2B	-388.699134	-388.826301	-388.814069	-388.837238
				-388.799864	-388.893849

^a Total energies are given in a.u., bold font stands for the ground electronic state of the structure. ^b CI matrix of each state is built on its own MO obtained at the geometry optimized for this state. The energies of two lower 2A states are presented for *c*-DEC⁺⁺.

relative energies of respective vertical cation states. At the geometry of neutral parent molecules, for both the isomers, there are two close in energy RC states whose single occupied MOs (SOMOs) are formed by symmetric combinations of components of the degenerate cyclohexane e_g MO. For *t*-DEC⁺⁺ these states belong to different representations of symmetry group of a neutral molecule, C_{2h} (2B_g and 2A_g). For *c*-DEC⁺⁺ (C_2 symmetry) both the states are totally symmetric, 2A . Note that the energy level of the next *c*-DEC⁺⁺ state, 2B , is also rather low.

For each isomer at the ROHF level geometry optimization of the states of different symmetry leads to two stationary structures that possess the same spatial symmetry but differ in the symmetry of the ground electronic state: C_{2h} (2A_g) and C_{2h} (2B_g) for *t*-DEC⁺⁺ and C_2 (2A) and C_2 (2B) for *c*-DEC⁺⁺. Single-point ROHF calculations of lower excited states performed for these structures by a change in initial guess reveal a crossing of the 2B_g and 2A_g terms of *t*-DEC⁺⁺ and 2A and 2B of *c*-DEC⁺⁺ as well. The terms crossing is preserved also at the CIS//ROHF level of calculations (Table 1). The crossing avoidance occurs along the pseudorotation coordinate via symmetry reduction to the nearest subgroup in which the crossing states belong to the same irreducible representation ($C_{2h} \rightarrow C_i$ for *t*-DEC⁺⁺ and $C_2 \rightarrow C_1$ for *c*-DEC⁺⁺) that allows the RC electronic state to change smoothly.

Thus, according to the data of ROHF and CIS calculations, the PESes of RCs of the isomeric decalins are the surfaces of conical intersection. Such a shape of adiabatic PES is typical for highly symmetrical Jahn–Teller active ions^{13,14} as well as for some of their low-symmetric derivatives containing substituents which slightly perturb the degenerate MO.^{15,16} A priori a similar PES structure is hardly to be expected for the RC of minimally symmetric decalin molecules because their SOMO are not perturbed components of the cyclohexane e_g MO but represent combinations of these components and are delocalized over both the rings (Figure 2).

The geometries of the *c*-DEC⁺⁺ and *t*-DEC⁺⁺ structures optimized by the ROHF method were further used as starting ones in the UB3LYP calculations. According to the data obtained at this calculation level as well, there are two structures for each RC (C_{2h} for *t*-DEC⁺⁺ and C_2 for *c*-DEC⁺⁺) with the ground states of different symmetry. The results of detailed PES study for these RCs are summarized in Table 2 and Figure 3.

Let us first consider the results for *t*-DEC⁺⁺, which is of a greater interest with respect to ESR data. The stationary structures of this RC form a pseudorotation cycle (Figure 3a). The C_{2h} (2A_g) structure **1** with an elongated central C–C bond corresponds to a PES minimum while C_{2h} (2B_g), **4**, where this bond is shortened, corresponds to a saddle point. An active coordinate at this point is similar to the pseudorotation mode of cyclohexane RC and has the same symmetry (b_g) but includes both the rings (Figure 4). Geometry distortion along the b_g mode in positive and negative directions leads to two equivalent mirror-symmetric C_i structures **3** that correspond to the PES minima and are related to C_{2h} (2A_g) structure via equivalent transition states **2** of C_i symmetry. Note that these structures are transition states for the central C–C bond stretching. Symmetry reduction $C_{2h} \rightarrow C_i$ mixes the 2A_g and 2B_g states that within the C_i group belong to the same totally symmetric representation. This results in a smooth change in the SOMO when moving along the pseudorotation path (Figure 5).

The *t*-DEC⁺⁺ PES is highly flattened (Table 2, Figure 5). According to calculation data the energy barrier between the mirror-symmetrical structures **3** is extremely low, 0.19 kcal/mol, which is comparable with the calculation accuracy. Regarding the ESR data, it suggests the complete averaging of hfc constants between the structures **3** even at 4.2 K. Calculated for this case a_H values agree well with the experimental ones observed in *c*-C₆F₁₁CF₃. Note that if the barrier does not exist, i.e., structure **4** corresponds to the PES minimum, the hfc

TABLE 2: Stationary PES Structures of *trans*- and *cis*-Decalin Radical Cations (UB3LYP/6-31G*)^a

structure	state	PES point	E_{tot} , au	E_{rel} , kcal/mol	R , Å ^b	a_{H} , G		
						calcd	exptl ^c	
<i>t</i> -DEC ⁺⁺								
1	C_{2h}	2A_g	min	-391.325871	0.15	1.847	53.1 (4H)	52.2 (4H)
2	C_i	2A_g	TS	-391.323325	1.74	1.642		
3	C_i	2A_g	min	-391.326104	0	1.509	33.5 (4H) ^d	34.6 (4H)
4	C_{2h}	2B_g	TS	-391.325801	0.19	1.502	38.6 (4H)	
<i>c</i> -DEC ⁺⁺								
1	C_2	2A	min	-391.322795	0	1.851	53.5 (2H), 48.9 (2H)	50.3 (4H)
2	C_2	2A	TS	-391.319861	1.84	1.598		
3	C_2	2A	min	-391.320297	1.57	1.525		
4	C_1	2A	TS	-391.312446	6.49	1.513		
5	C_1	2A	min	-391.312575	6.41	1.523		
6	C_2	2B	TS	-391.306118	10.46	1.502		

^a We omit here the values of zero-point energy corrections because the harmonic approximation may result in large error in the Hessian calculations for shallow flattened minima. ^b R stands for the central C–C bond length. ^c The data is obtained in ref 4. ^d The value is obtained by averaging over two equivalent minima, corresponding to mirror-symmetrical C_i structures **3** with hfc constants $a_{\text{H}} = 50.4$ (2H) and $a_{\text{H}} = 16.5$ (2H) G. Including C_{2h} (2B_g) structure into the averaging, we obtain $a_{\text{H}} = 35.2$ (4H) G.

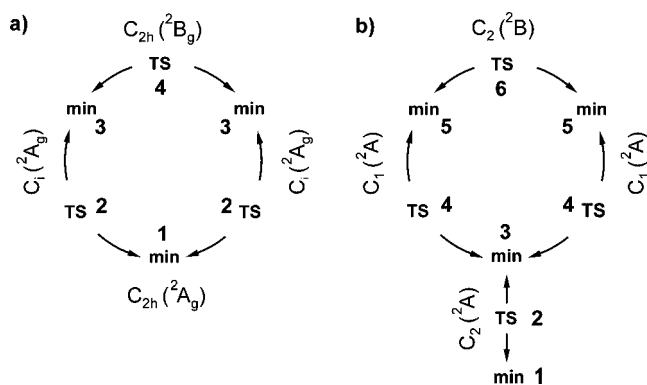


Figure 3. PES schemes for radical cations of *trans*- (a) and *cis*-decalin (b). The structure numbers correspond to Table 2.

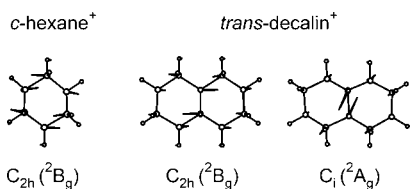


Figure 4. Pseudorotation modes at the PES saddle points of the cyclohexane and *trans*-decalin radical cations.

constants do not change significantly and agree with the ESR data as well (Table 2).

In any case, we may consider the PES to have two minima (the structure **1** and a wide shallow minimum joining the structures **3** and **4**), which are separated by two equivalence transition states (mirror-symmetrical structures **2**). The energies at the PES minima are very close to each other, which is in a good agreement with the data on a simultaneous observation of two RC states at 4.2 K.⁴ Calculations reproduce well the experimental hfc constants for both ESR spectra observed for *t*-DEC⁺⁺ (Table 2). The small (1.74 kcal/mol) height of energy barrier for pseudorotation conforms to the data on the spectral exchange with the temperature increase.^{4,8} In particular this value corresponds to the exchange rate constant estimated from the 77 K ESR spectrum.

A distinctive feature of *c*-DEC⁺⁺ PES structure (see Figure 3) is that the C_2 (2A) structure **1** with an elongated central bond C–C, which corresponds to the global PES minimum, is beyond the pseudorotation gutter. The motion along the pseudorotation

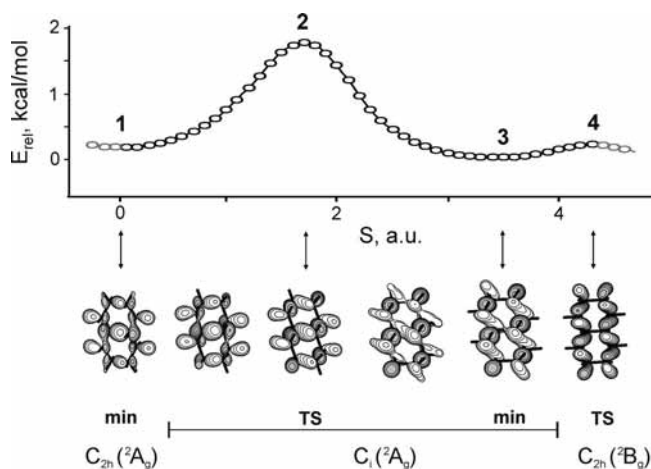


Figure 5. The PES section of the *trans*-decalin radical cation along the pseudorotation path (half of the cycle) and respective SOMO evolution.

coordinate from the transition state C_2 (2B), **6**, through asymmetric C_1 structures **5** and **4** (Figure 3b) leads to another C_2 (2A) structure **3** with a noticeably shorter central bond (Table 2). Structures **1** and **3** are related via the transition state of the central C–C bond stretching (**2**). Their SOMO are of the same symmetry but differ by the density distribution. Because of both the small (comparable with the calculation accuracy) depth of *c*-DEC⁺⁺ PES minima, except the global one, and relatively large height of the pseudorotation barrier, only structure **1** is observed in the ESR experiments. a_{H} constants calculated for this structure are in fair agreement with the experimental ones (Table 2). Insignificant nonequivalence of calculated hfc constants for two groups of protons is less than the linewidth in experimental ESR spectra.⁴

4. Conclusion

Our study shows that adiabatic PESes of the radical cations of low-symmetric *cis*- and *trans*-decalin molecules are the surfaces of pseudorotation that results from the avoided crossing. The maximal height of the barrier for pseudorotation is less than 2 kcal/mol for *t*-DEC⁺⁺ and about 9 kcal/mol for *c*-DEC⁺⁺. Unlike *t*-DEC⁺⁺, whose stationary structures are entirely involved in pseudorotation, the *c*-DEC⁺⁺ structure of minimum energy lies beyond the pseudorotation gutter. The results of

calculations are in good agreement with the experimental ESR data. Thus, the difference in spectral behavior of these isomeric radical cations is completely determined by the distinctions revealed in their PES structures.

Acknowledgment. We are grateful to Professor Yu. N. Molin who has attracted our attention to these interesting and unusual radical cation systems. This work was supported by the Russian Foundation for Basic Research (Grant Nos. 07-03-00576 and 08-03-00495).

References and Notes

- (1) Carey, F. A.; Sandberg, R. J. *Advances Organic Chemistry, Part. A*; Plenum Press: New York, London, 1977.
- (2) Shida, T.; Takemura, Y. *Radiat. Phys. Chem.* **1983**, *21*, 157.
- (3) Iwasaki, M.; Toriyama, K.; Nunome, K. *Faraday Discuss., Chem. Soc.* **1984**, *78*, 19.
- (4) Melekhov, V. I.; Anisimov, O. A.; Sjoqvist, L.; Lund, A. *Chem. Phys. Lett.* **1990**, *174*, 95.
- (5) Werst, D. W.; Percy, L. T.; Trifunac, A. D. *Chem. Phys. Lett.* **1988**, *153*, 45.
- (6) Trifunac, A. D.; Werst, D. W.; Percy, L. T. *Radiat. Phys. Chem.* **1989**, *34*, 547.
- (7) Barnabas, M. V.; Trifunac, A. D. *Chem. Phys. Lett.* **1991**, *187*, 565.
- (8) Tadjikov, B. M.; Stass, D. V.; Molin Yu., N. *J. Phys. Chem. A* **1997**, *101*, 377.
- (9) Toropov, Yu. V.; Sviridenko, F. B.; Stass, D. V.; Doktorov, A. B.; Molin, Yu. N. *Chem. Phys.* **2000**, *253*, 231.
- (10) Borovkov, V. I.; Molin Yu., N. *Phys. Chem. Chem. Phys.* **2004**, *6*, 2119.
- (11) Schmidt, M. W.; Baldrige, K. K.; Boatz, J. A.; Elbert, S. T.; Gordon, M. S.; Jensen, J. H.; Koseki, S.; Matsunaga, N.; Nguyen, K. A.; Su, S. J.; Windus, T. L.; Dupuis, M.; Montgomery, J. A. *J. Comput. Chem.* **1993**, *14*, 1347.
- (12) Laikov, D. N. *Chem. Phys. Lett.* **1997**, *281*, 151.
- (13) Bersuker, I. B.; Polinger, V. Z. *Vibronic Interactions in Molecules and Crystals*; Springer-Verlag: Berlin, 1989.
- (14) Bersuker, I. B. *Chem. Rev.* **2001**, *101*, 1067.
- (15) Beregovaya, I. V.; Shchegoleva, L. N. *Int. J. Quantum Chem.* **2002**, *88*, 481.
- (16) Vysotsky, V. P.; Salnikov, G. E.; Shchegoleva, L. N. *Int. J. Quantum Chem.* **2004**, *100*, 469.

JP807568G